Research Square

Preprints are preliminary reports that have not undergone peer review.
They should not be considered conclusive, used to inform clinical practice,
or referenced by the media as validated information.

Synergistic Effects of Paederia Foetida Fiber and Mahogany Fruit Husk Filler on the Mechanical, Thermal, Acoustic Performance of Polyester Biocomposites

Nasmi Herlina Sari

n.herlinasari@unram.ac.id

University of Mataram

Suteja Suteja

University of Mataram

Muhammad Nabil Fadhlurrohman Rivlan

University of Mataram

Apip Amrullah

University of Lambung

Research Article

Keywords: Biocomposites, Paederia foetida fibers, mahogany fruit husk, acoustic absorption, Thermal stability

Posted Date: May 5th, 2026

DOI: https://doi.org/10.21203/rs.3.rs-9602925/v1

License: This work is licensed under a Creative Commons Attribution 4.0 International License.
Read Full License

Additional Declarations: No competing interests reported.

Abstract

Sustainable multifunctional composites are gaining popularity as a replacement for traditional synthetic materials. This study explores at how *Paederia foetida* fiber (PFs) reinforcement and mahogany Fruit Husk (MP) filler work together to improve the mechanical, thermal, acoustic, and morphological aspects of polyester-based composites. Tensile and flexural testing, sound absorption tests, thermogravimetric analysis (TGA), and scanning electron microscopy (SEM) were used to characterize the composites made with various volume fractions. The results show a significant improvement in mechanical efficiency, with tensile strength increasing from 38.71 MPa to 63.2 MPa and elastic modulus increasing from 1573.43 MPa to 1892.31 MPa, as well as a drop in elongation from 3.81% to 2.25%, showing improved stiffness. Flexural strength and modulus also rose at around 105 MPa and 3.2 GPa, respectively. The composites effectively absorbed sound in the mid-to-high frequency range, reaching a maximum absorption coefficient of 0.539 at 4000 Hz. Thermal study revealed higher stability, with a highest degradation temperature of 402.47°C and char residue up to 5.72%. SEM examinations revealed enhanced interfacial bonding and fewer vacancies. These findings reveal a synergistic reinforcement process and emphasize the composites' potential for use in lightweight structural panels, vehicle interior components, building acoustic insulating material, and environmentally friendly sound-absorbing materials.

1. Introduction

The increased need for environmentally friendly and high-performance materials has expedited the emergence of natural fiber-reinforced polymer composites as potential substitutes for traditional synthetic materials [1, 2] Natural fibers have characteristics like a light density, biodegradability, renewability, and cost-efficiency, which make them increasingly appealing for lightweight structural purposes. Recent research indicates that natural fiber composites can efficiently replace imitations in automotive, construction, and engineering uses while preserving competitive mechanical properties and environmental benefits [3]. In this context, the creation of hybrid composites that include both natural fibers and particle fillers has emerged as a promising technique for improving multifunctional performance.

Paederia foetida, a natural fiber with fibrous architecture and availability in tropical locations, has received little attention despite its promise as a reinforcement material [4, 5]. Meanwhile, lignocellulosic biomass waste, such as mahogany (*Swietenia macrophylla*) fruits husk, is a viable filler, thanks to its high lignin concentration, which helps with rigidity, thermal stability, and char production [6]. The use of biomass-derived fillers has been found to improve composite stiffness and thermal resistance while maintaining environmental benefits. Building on this potential, the combination of natural fibers and biomass fillers is projected to have synergistic effects by improving interfacial bonding and stress transfer efficacy [7].

Previous research has shown that better fiber-matrix interaction greatly improves mechanical properties, whilst the addition of particle fillers increases stiffness and dimensional stability. Natural fiber composites, on the other hand, show promising acoustic qualities because of their porous and fibrous structure, which allows for sound absorption via viscous and thermal dissipation mechanisms [8]. Recent studies demonstrate that increasing fiber content and optimizing internal structure increases sound absorption performance, particularly in the mid-to-high frequency range [9, 10]. However, the majority of present research focuses on either mechanical and acoustic performance independently, with only a few studies investigating the overall multifunctional behavior of hybrid composites integrating fiber reinforcement and biomass fillers. As a result, a thorough knowledge of the link between microstructure and multifunctional characteristics remains an important research gap.

The behavior of natural fiber composites is heavily influenced by microstructural variables like interfacial bonding, filler dispersion, and vacancy distribution. These characteristics affect not just mechanical strength, but also thermal degradation and acoustic performance [11, 12]. Thermal stability, for example, is intimately tied to the breakdown of hemicellulose, cellulose, components, and also the presence of fillers that might promote char formation and slow degradation. Furthermore, recent research shows that hybrid reinforcement techniques can improve thermal and acoustic properties by increasing structural integrity and reducing polymer chain mobility [13]. To overcome these restrictions, a more comprehensive method that considers morphology, mechanical properties, thermal stability, and sound quality is necessary.

Therefore, the goal of this study is to create and analyze polyester composites strengthened with *Paederia foetida* fiber (PFs) and filled with mahogany fruit husk (MP). The study focuses on determining tensile and flexural parameters, sound absorption behavior, thermal stability using thermogravimetric analysis, and fracture morphology using SEM. This study aims to create a thorough structure-property link in hybrid natural composites by systematically comparing microstructural aspects with macroscopic performance. Finally, the integration of mechanical, thermal, acoustic, and morphological evaluations into a single composite system based on underutilized natural resources distinguishes this study. This technique sheds new light on the design of sustainable multifunctional materials and helps to promote eco-friendly composite innovations for structural and acoustic purposes.

2. Materials and Methods

2.1. Materials

The polymer matrix consisted of unsaturated polyester resin (UPR). Methyl ethyl ketone peroxide (MEKP) was utilized as the curing initiator, with cobalt naphthenate as the accelerator. *Paederia foetida* fibers were gathered in Sekarbela, Mataram, West Nusa Tenggara Indonesia.

Before being treated, the fibers were hand removed, cleaned to remove contaminants, and air-dried, as illustrated in Fig. 1a. The husk of mahogany fruit is extracted from local wood processing waste, and the

skin is cut and ground into a fine powder before being sieved through 200 mesh to produce a powder that measures 75 µm, as shown in Fig. 1b.

Figure 1. Extraction and preparation of (a) *Faederia foetida* fibers, (b) Mahongany fruit husk powders

2.2. NaOH Treatment of PFs

The *Paederia foetida* fibers were subjected to alkali treatment to improve interfacial bonding. The fibers were immersed in a 5 wt% NaOH solution for 2 h at room temperature (27 ^{o}C), then thoroughly washed with distilled water until neutral pH was achieved. The reaction of fibers and mahogany fruits husk in NaOH following Eq. 1 and Eq. 2 [14]. The treated fibers and Mahogany powders were dried in an oven at 60°C for 1 h. Further, the treated fibers called PFs, and mahogany fruits husk powder called is MP.

$$Paederia\ f.\ \text{fiber} - \text{OH} + \text{NaOH} \rightarrow \text{fiber} - \text{O}^- + \text{Na}^+ + \text{H}_2\text{O}$$

1

$$\text{Mahogany fruits husk powders} - \text{OH} + \text{NaOH} \rightarrow \text{MP powders} - \text{O}^- + \text{Na}^+ + \text{H}_2\text{O}$$

2

2.3. Composite Fabrication

Hand lay-up was used to create polyester composites, which were then hot-pressed. The PFs were utilized as reinforcement with a set weight fraction (20 wt%), and MP was used as filler at different loadings (0, 2.5, 5, and 10% vol.), as displayed in Table 1. To guarantee consistent dispersion, mechanical stirring was used to combine the polyester resin with MP filler. Then, MEKP (1 wt%) was added. The PFs were then added to the mixture at random. The mixture was put into a mold and pressed at 5 MPa for 24 h at room temperature. Post-curing was done at 70°C for 2 h.

Table 1
The ratio of PFs and MP in different bio composites.

Sample codes	Vol. Fraction (%)		
	Paederia f. fibers	Unsaturated resin polyester (UPR)	Mahogany fruits husk powder (MP)
SA	20	80	0
ST		77.5	2.5
UD		75	5
UN		70	10

2.4. Characterization

2.4.1. Tensile Test

Tensile characteristics were measured in accordance with ASTM D3039 [15] on a universal testing machine (UTM) (model RTG 1310 INSTRON). The experiments were conducted at a crosshead speed of 5 mm/min in an ambient laboratory setting (temperature: 25 ± 2°C, relative humidity: 61%). Tensile strength, modulus, and elongation at break were measured. Each composition was evaluated using at least five specimens, and the average values and standard deviations were given.

2.4.2. Flexural Test

Flexural characteristics were determined using a three-point bending setup in accordance with ASTM D790 and computed using Eq. (3)[16]. The tests were conducted on the same universal testing machine outfitted with a flexural fixture. Specimens had measurements of 127 mm × 12.7 mm × 3 mm. The crosshead speed was set to 2 mm/minute. Flexural strength and modulus were calculated from load-deflection curves. A minimum of five specimens from each sample group were tested.

$$\sigma_f = \frac{3.F.L}{2.b.d^2}$$

3

Where, σ_f = flexural strength (MPa), F = the maximum load a specimen can receive before fracture (N), L = support span between two support (mm), b = Specimen width (mm), d = specimen thickness (mm).

2.4.3. Density test

In compliance with ASTM D792 [17], the Archimedes principle was used to calculate the density of the composite samples. Rectangular specimens of roughly 20 mm x 20 mm x 5 mm were made. The materials were dried and weighed in air (W_a) before being submerged in distilled water to determine their immersed weight (W_w). To guarantee measurement accuracy, care was taken to eliminate surface air bubbles. The following formula 4 was used to get the density (ρ):

$$\rho = \frac{W_a}{W_a - W_w} x \rho_{water}$$

4

where W_a is the weight in air (g), W_w is the weight in water (g), ρ is the density of the composite (g/cm³), and $\rho_{(water)}$ is the density of water (usually 0.997 g/cm³ at ambient temperature).

At least three repetitions of each measurement were made at room temperature, and the average values together with standard deviations were reported.

2.4.4. Thermogravimetric Analysis (TGA)

The thermal stability of the composites was investigated using a Metler Toledo Instruments thermogravimetric analysis (TGA) under a nitrogen environment, heating from room temperature to 1000°C at a rate of 10°C/min [18].

2.4.5. Morphological test

Scanning electron microscopy (SEM) was used to investigate the biocomposites' fracture surfaces following tensile testing. To increase conductivity, samples were sputter-coated with a small layer of gold before observation.

2.4.6. Airflow Resistivity

The airflow resistivity (AR) of the composite samples was determined to assess their resistance to air flow, which is an important parameter in determining acoustic energy dissipation in porous materials. The ISO 9053-compliant steady-state airflow method was used for the test. Disc-shaped specimens with a diameter of 100 mm to match the impedance tube and a thickness of 10 mm were manufactured [19]. A regulated airflow was directed through the sample, and the pressure decrease across the specimen was measured. The AR was determined as the ratio of pressure differential to airflow velocity, normalized by sample thickness. The composites' internal friction behavior was analyzed using the loss factor (tan δ), which represents the material's ability to dissipate vibrational energy. This parameter was determined using dynamic mechanical analysis (DMA) with oscillatory loading conditions. Rectangular specimens were examined in three-point bending mode at a frequency of one Hz over a temperature range of 120 ^{o}C [20]. The loss factor (tan δ) was calculated as the ratio between loss modulus and storage modulus. To assure data reliability, all measurements were taken at room temperature and repeated at least three times, with average values reported.

2.4.7. Sound Absorption Test

The impedance tube method, as described in ASTM E1050, was used to analyze the composites' sound absorption capabilities [21]. The measurements were made with a two-microphone impedance tube system (B&K Type 4189-A-021) that can determine the normal incidence sound absorption coefficient from 100 to 4000 Hz. Circular specimens with diameters match the inner diameter of the impedance tube were made, as well as thicknesses of 10 mm. The samples were carefully put into the sample holder to eliminate air gaps that could degrade measurement accuracy.

3. Results and Discussion

3.1. Tensile strength analysis

Figure 3 depicts the mechanical strength of PF/MP reinforced composites. Tensile properties improve from SA to UN, with tensile strength increasing from 38.71 ± 2.65 MPa to 63.2 ± 2.1 MPa and elongation at break decreasing from 3.81 ± 0.63% to 2.25 ± 0.3%. Elastic modulus also increases from 1573.4 ± 76 MPa to 1892.3 ± 60 MPa. Figure 3a shows a steady improvement in tensile strength (46.4 ± 2.12 MPa for

ST and 58.6 ± 1.65 MPa for UD), indicating improved stress transfer efficiency among the polyester matrix, PFs, and MP filler. This increase is related to improved interfacial bonding, which allows for more effective load distribution and delays failure. The presence of PFs reinforcement serves as the principal load-bearing mechanism, whilst the addition of particulate filler increases matrix stiffness and limits polymer chain mobility. A similar trend has been seen, where enhanced interfacial bonding lowers fiber pull-out and improves load transfer, resulting in increased tensile strength [22]. The UN sample had the maximum tensile strength (63.2 ± 2.1 MPa), indicating optimal fiber-filler hybridization. This behavior can be linked to a synergistic reinforcing mechanism in which PFs operate as stress transporters while fillers fill voids, minimizing stress concentration locations and enhancing structural integrity. Previous research has shown that proper mixtures of natural fibers and fillers improve mechanical performance through better dispersion and interfacial adhesion [23].

Conversely, the drop in elongation from 3.81% (SA) to 2.25% (UN) (Fig. 3b) indicates greater brittleness. This behavior is usually related with the use of hard fillers, which limit plastic deformation and impair composite ductility [22]. The stiffness increase (modulus from 1573 MPa to 1892 MPa) (Fig. 3c) reinforces this trend, as hard particles limit matrix deformation and improve resistance to elastic strain. Similar findings show that adding filler increases stiffness but may diminish tensile deformability because to limited molecular mobility [24].

Mechanistically, the observed trend can be explained by three primary factors: (i) improved interfacial adhesion, which improves load transfer; (ii) filler-induced stiffening, which increases modulus while decreasing ductility; and (iii) reduced void content, which leads to more consistent mechanical response, as evidenced by the low standard deviation values in Fig. 3. However, it is vital to highlight that such enhancements are usually valid up to an ideal composition. Excessive filler or inadequate dispersion can cause agglomeration and weak interfacial areas, compromising tensile characteristics, as seen in natural fiber composites with increased reinforcement content [25]. Overall, these findings demonstrate that the hybridization of PFs and MP improves tensile strength and stiffness while decreasing ductility, which is typical of rigid particle-reinforced composites.

3.2. Flexural strength analysis

Flexural strength and modulus gradually rise over all composite modifications, as seen in Figs. 4a-b. Flexural strength increases from roughly 65 MPa for SA to around 78 MPa for ST, then to about 92 MPa for UD, and finally to nearly 105 MPa for UN. The flexural modulus follows a similar pattern, increasing from around 2.1 GPa for SA to 2.5 GPa for ST, then 2.8 GPa for UD, and finally 3.2 GPa for UN. This continuous rise in both parameters shows that the PFs/MP composite system is more resistant to bending deformation and stiffer. The increased flexural strength (Fig. 4a) is due to a more effective stress transfer mechanism, notably in the specimen's outer layers, where tensile and compressive stresses are highest during bending. The addition of PFs improves load-bearing performance, whereas MP improves stress distribution within the matrix. This combination impact promotes increased interfacial adhesion, reduces fiber pull-out, and allows for more stress accommodation before failure.

Recent composite systems have shown comparable characteristics, with enhanced fiber-matrix interaction leading to significant increases in flexural strength and the structure [26].

The steady increase in flexural modulus (Fig. 4b) supports the stiffening effect caused by hybrid reinforcement. The presence of stiff filler particles limits polymer chain mobility, resulting in lower elastic deformation under load. As the composition proceeds toward the UN sample, the composite's structure becomes more compact and rigid, as seen by increasing modulus values. This behavior is consistent with previous research showing that the addition of particle fillers increases stiffness by restricting matrix deformability and enhancing load transmission efficiency [27].

The observed trend further implies that the combination of PFs and MP results in a synergistic reinforcement effect, with fibers largely supporting bending loads and filler particles occupying microvoids and preventing crack propagation. This interaction not only increases mechanical performance, but it also helps to distribute stress more uniformly throughout the composite. Furthermore, the presence of finely dispersed filler likely decreases internal voids and increases stress distribution, resulting in greater bending resistance. Similar investigations have found that appropriate filler loading improves flexural strength and modulus due to increased packing density and interfacial adhesion, whereas excessive MP can cause agglomeration and performance loss. According to fracture mechanics, the integrated reinforcing delays crack start and propagation under bending loads. The fibers serve as crack-bridging elements, whilst the filler particles impede fracture growth by forming tortuous crack channels, boosting energy absorption before failure. Overall, the results show that increasing reinforcing complexity from SA to UN significantly improves flexural strength and modulus, proving the efficiency of hybrid PFs and MP.

3.3. Density analysis

The density of the developed biocomposites are presented in Fig. 5, showing a declining trend from SA (1.37 g/cm³) to UN (1.02 g/cm³), suggesting that the composites' internal structure and porosity are gradually changing. While the lower density in UN indicates increased porosity and decreased packing efficiency of the fiber-filler system, the higher density in SA denotes a more compact structure with minimal void content. From a microstructural standpoint, void creation during fabrication, filler incorporation, and fiber distribution all have a significant impact on density. Tighter matrix packing and less pore connectivity, which limit internal routes for air and acoustic wave propagation, are indicated by SA's comparatively high density.

On the other hand, the progressive decrease in density toward UN indicates the development of a more porous and convoluted structure, probably as a result of better fiber and filler particle dispersion that creates micro-voids and interfacial gaps. Acoustic behavior is directly affected by this trend. Higher porosity in lower density materials generally permits deeper sound wave penetration and improved energy dissipation via viscous and frictional losses. Despite enhanced stiffness, an excessively high density can restrict the entry of sound waves, decreasing the efficiency of absorption. On the other hand, a balance between internal friction and airflow resistance is made possible by an ideal intermediate

density, which is necessary for efficient sound absorption. Moreover, the mechanical–acoustic trade-off is also influenced by density. This behavior is in line with previous research showing that in natural fiber composites, density, porosity, and fiber packing greatly influence mechanical integrity and acoustic absorption [13].

3.4. Airflow resistivity (AR) and and Viscoelastic Behavior

Airflow resistivity (AR), viscoelastic characteristics, and the composites' acoustic performance are clearly correlated, as shown by the results in Table 2. The ST sample has the highest loss modulus (63.9 MPa), damping factor (tan δ = 0.045), and airflow resistivity (12,800 Pa·s/m²). This combination shows an ideal balance between internal energy dissipation and airflow resistance, which facilitates the efficient conversion of acoustic energy into heat via viscous and frictional mechanisms. As a result, this sample has the highest sound absorption coefficient ever measured.

The SA sample, on the other hand, has a poor damping capacity (tan δ = 0.021) due to its modest loss modulus (26.3 MPa) and airflow resistivity (4,500 Pa·s/m²). While the decreased viscoelastic dissipation further limits energy loss, the low AR implies that sound waves can travel through the material with little contact. This accounts for SA's subpar acoustic performance, especially at low and medium frequencies. With airflow resistivity values of 6,900 and 9,800 Pa·s/m², respectively, the UD and UN samples show intermediate behavior. In comparison to SA, increased internal friction is indicated by the corresponding increases in tan δ (0.028–0.036) and loss modulus (37.8–49.7 MPa).

Notably, the UN sample strikes a better balance between damping capacity and stiffness (E' = 1380 MPa), supporting consistent sound absorption performance over a larger frequency range. This implies that adequate tortuosity for acoustic wave attenuation is maintained while avoiding excessive densification. From a mechanical standpoint, the viscoelastic parameters regulate the effectiveness of energy dissipation inside the material, whereas airflow resistivity controls the degree of interaction among incident sound waves and the porous structure. While higher loss modulus and tan δ improve frictional dissipation at the fiber–matrix and filler interfaces, high AR increases viscous losses because it restricts air movement. On the other hand, an overly high density could hinder the penetration of sound waves by decreasing pore connection.

As a result, the ST sample's higher performance suggests the existence of an ideal microstructure with strong interfacial contacts, linked porosity, and sufficient airflow resistance.

Table 2
Airflow resistivity, and internal friction of PFs/MP biocomposites

Sample	Airflow Resistivity (Pa·s/m²)	Storage Modulus, E' (MPa)	Loss Modulus, E'' (MPa)	Internal Friction (tan δ)
SA	4,500 ± 320	1250 ± 60	26.3 ± 2.1	0.021 ± 0.002
ST	12,800 ± 540	1420 ± 75	63.9 ± 3.8	0.045 ± 0.003
UD	6,900 ± 410	1350 ± 68	37.8 ± 2.6	0.028 ± 0.002
UN	9,800 ± 470	1380 ± 70	49.7 ± 3.1	0.036 ± 0.003

3.5. Sound absorption analysis

Figure 6 shows that the absorption coefficient (α) increases dramatically with frequency for all composite variation, with low values at 125 Hz and gradually larger values at mid-high frequencies. This pattern is consistent with porous and natural fiber-based composites, which often have poor low-frequency absorption but better performance at higher frequencies due to increased viscosity and thermal dissipation mechanisms [28]. ST consistently has the maximum absorption capability across the frequency range, with values ranging from 0.346 at 250 Hz to 0.539 at 4000 Hz, suggesting greater acoustic energy dissipation. Conversely, SA shows the lowest performance, with α growing from 0.1127 to 0.3869, while UD and UN demonstrate moderate behavior, with highest values of 0.4340 and 0.4544 at 4000 Hz. Most samples meet the threshold of α ≥ 0.2 at frequencies ≥ 500 Hz, showing effective sound absorption capabilities in the mid-to-high frequency range, a usual criterion for acoustic materials.

The ST sample's higher performance implies an ideal balance between PF structure and MP distribution, which improves airflow resistivity and internal friction inside the composite. The presence of PFs fibers creates a porous network that allows sound waves to pass through the material, while the mahogany powder filler increases surface area and facilitates energy dissipation via viscous losses. As sound waves travel through the composite, repetitive air particle oscillations cause friction with pore walls, turning acoustic energy into heat, which is the principal mechanism of sound absorption [10].

Shorter wavelengths at larger frequencies are more easily dampened within the porous structure, which explains the increase in absorption with frequency. Low frequencies (125–250 Hz) have a large wavelength compared to material thickness, resulting in minimal interaction between sound waves and interior structure, leading in low α values. This phenomenon is extensively described in natural fiber composites, where thickness and porosity are important factors in low-frequency absorption ability [10, 17]. The discrepancy between UD, UN, and ST suggests that excessive filler or poor dispersion may lower acoustic efficiency. While MP increases stiffness and internal friction, high load reduces pore connection, limiting sound wave entry and decreasing energy dissipation efficiency. Similar findings have been reported, where hybrid natural fiber composites exhibit best acoustic performance at specified compositions, after which agglomeration and reduced porosity have a negative impact on absorption [8]. Overall, the results show that PF-MP hybridization significantly improves sound absorption efficiency,

especially at medium and high frequencies, with the ST design exhibiting the most effective acoustic behavior because of its balanced microstructure and improved energy dissipation mechanisms.

.

3.6. Morphology of composites by SEM

The fracture surface morphology in Figs. 7a-d shows a distinct evolution of interfacial properties and failure mechanisms as reinforcement complexity increases. In SA (Fig. 7a), the surface is dominated by fiber pull-out, smooth fiber surfaces, and obvious gaps between fiber and matrix, indicating weak interfacial adhesion. The existence of voids and debonded regions indicates inefficient stress transmission, which is consistent with earlier observations of inferior tensile and flexural characteristics, as well as reduced acoustic absorption due to inadequate internal energy dissipation routes. In contrast ST, on the other hand (Fig. 7b), has a rougher fracture surface, less fiber pull-out, and more matrix adherence on fiber surfaces, showing better interfacial bonding. The fibers appear to be more immersed in the matrix, indicating better load transmission efficiency. This morphology reflects the previously observed improvement in tensile and flexural capabilities, as well as the best sound absorption performance, which can be ascribed to a more interconnected microstructure that enhances internal friction and acoustic energy dissipation [29]. Further UD sample (Fig. 7c) shows further refinement, with the fracture surface becoming more compact, with fewer voids and greater filler dispersion. The presence of attached matrix fragments and fractured fibers rather than pulled-out fibers suggests that failure is caused by fiber fracture rather than interfacial debonding, indicating higher interfacial adhesion. This shift is consistent with further stiffness and strength gains, and also improved acoustic behavior caused by more uniform pore distribution and increased tortuosity for sound wave attenuation.

The UN sample (Fig. 7d) has the most integrated structure, with few voids, good fiber-matrix interlocking, and signs of fracture bridging and fiber breakage. The rough and irregular fracture surface indicates greater energy absorption during fracture, which accounts for the higher tensile and flexural strength values published previously. However, the denser structure may diminish pore connectivity compared to ST, explaining why, while acoustic absorption is superior to SA, it does not outperform ST at certain frequencies [13]. In addition, mechanistically, the observed morphological history shows a shift from interfacial debonding-dominated failure (SA) to fiber breaking and crack-bridging mechanisms (UN). The use of mahogany powder filler helps to fill voids, improve stress distribution, and increase interfacial contact area, while PFs serve as the major load-bearing framework. Similar results have been reported in recent research, where better fiber-matrix adhesion and appropriate filler dispersion improve mechanical performance while impacting acoustic behavior via changes in porosity and internal structure [8][10]. The SEM data substantially support the mechanical and acoustic results, demonstrating that the synergistic interaction of PFs and MP filler improves interfacial bonding, decreases flaws, and alters fracture mechanisms, resulting in improved composite performance.

3.7. Thermogravimetric Analysis

Figure 8a-d depicts the thermogravimetric behavior of the composites, which display a typical multi-stage degradation appearance of lignocellulosic fiber-reinforced polyester. All samples show a first small weight loss at low temperatures, followed by a major degradation stage in the 250–450°C range, which corresponds to the disintegration of hemicellulose, cellulose, and polyester [27, 28]. There is a notable variance in deterioration behavior among the samples. The SA composite (Fig. 8a) exhibits a relatively sharp mass loss throughout the primary deterioration stage, indicating reduced thermal stability and less interfacial bonding, allowing for rapid thermal disintegration. In contrast, the ST sample (Fig. 8b) shows a more progressive degradation slope, indicating higher thermal resistance due to improved interaction among fiber, filler, and matrix phases.

The UD composite (Fig. 8c) exhibits the greatest resistance to first degradation, as shown by the delayed commencement of mass loss. This finding is consistent with the highest Ton value given in Table 2 (351.70°C), indicating that better interfacial bonding and filler dispersion improve the composite structure's resilience during the early phases of thermal degradation. In hybrid natural fiber composites, such behavior has been linked to decreased volatile release and restricted polymer chain mobility [32]. In comparison, the UN sample (Fig. 8d) displays a little earlier deterioration commencement but has the highest thermal resistance throughout the primary decomposition stage. This trend is consistent with the T_{max} value provided in Table 2 (402.47°C), demonstrating that the composite can withstand rapid deterioration at high temperatures. The TGA curve also shows a greater residual mass at the end stage, which is supported by the residue value of 5.72% shown in Table 3. This increased char generation is owing to the lignin-rich MP, which decays across a wider temperature range and leads to carbonaceous residue formation.

Table 3
Thermal degradation behavior typical of natural fiber–polyester systems

Samples	T_{on} (°C)	Weight loss (wt %)	T_{max} (°C)	Weight loss (wt %)	Residue at 1000°C (%)
SA	325.74	4.37	377.23	89.82	2.86
ST	322.64	5.89	371.64	82.14	4.4
UD	351.70	6.81	391.65	87.53	5.01
UN	314.74	8.11	402.47	88.2	5.72

The discrepancies seen in Figs. 8a-d, combined with the quantitative results in Table 3, demonstrate that thermal stability is determined by a balance between PFs degradation and MP-induced stabilization. Because of their lignocellulosic character, PFs contribute to quicker degradation, whereas MP improves thermal resistance by increasing aromatic content, lowering mass loss rate, and boosting char formation. Recent investigations have shown that lignin-containing fillers improve heat stability and residual char production in natural fiber composites. Overall, the combined interpretation of TGA curves and tabulated data shows a synergistic thermal stabilization effect, with the UD sample showing

superior resistance to initial deterioration and the UN sample showing increased stability at higher temperatures and greater char formation. This behavior demonstrates the usefulness of hybrid reinforcement in changing breakdown pathways and increasing the high-temperature performance of polyester composites.

4. Conclusion

This study shows that the hybridization of PFs fiber with MP improves overall efficacy of polyester composites by utilizing synergistic reinforcement processes. The addition of PFs largely increases load-bearing capacity, whereas the MP filler improves rigidity, thermal resistance, and structural strength. The mechanical results demonstrate a significant improvement in tensile and flexural characteristics, coupled by decreased ductility, indicating a shift toward a stiffer and more rigid composite. Morphological observations show a transition from interfacial deformation and fiber pull-out to fiber breakage and strong interfacial bonding, resulting in increased stress transmission efficiency. Furthermore, the composites have good sound attenuation in the mid-to-high frequency range, indicating their potential as multifunctional materials. Thermal investigation reveals the presence of lignin-rich filler, which improves high-temperature resistance and increases char formation.

Despite these encouraging findings, numerous areas require further exploration. Future research should concentrate on improving filler loading and fiber pretreatment to balance mechanical performance with acoustic efficiency, especially at low frequencies where absorption is limited. Advanced surface modification approaches could be investigated to improve interfacial bonding and durability. Furthermore, long-term performance, such as environmental aging, resistance to water, and fatigue behavior, should be examined to assure dependability in real-world applications. To better understand the interplay between microstructure and macroscopic features, numerical modeling and multi-scale analysis should be used together. Overall, the proposed hybrid composite shows great promise as a sustainable multifunctional technology for use in real life, particularly lightweight structural panels, vehicle interior parts, and building acoustic insulation system. Its improved mechanical strength, thermal endurance, and sound absorption capability make it ideal for environmentally friendly engineering applications that require structural integrity as well as noise management.

Declarations

CRediT authorship contribution statement

N.H. Sari: Writing – original draft, Formal analysis, Methodology, Data curation, Conceptualization, Funding acquisition, Writing – review & editing.

S. Suteja: Methodology, Investigation, Formal analysis, Supervision, Validation

M.N. Fadhlurrohman Rivlan: Project administration, Software.

A. Amrullah: Writing – review & editing.

Declaration of competing interest

The authors state that there is no evidence of any competing financial interests or personal relationships influencing any of the work presented in this study.

Acknowledgements

The authors gratefully acknowledge the financial support provided by Ministry of Education, Culture, Research and Technology Indonesia under project Fundamental research No. 030/E5/PG.02.00.PL/2-23. The authors also thank the laboratory staff for their assistance in experimental work and material characterization. The support from University of Mataram in providing research facilities is highly appreciated.

Data availability

Data will be made available on request.

References

1. Lakshmaiya N, Kota SR, Bhaskar K, Palanivel A, Chukka NDKR, Maranan R (2025) Sustainable hybrid epoxy composites reinforced with Kenaf fiber banana peel waste and SiC for multifunctional performance. Results Eng 28:107558. 10.1016/j.rineng.2025.107558. September
2. Khalid MY, Al Rashid A, Arif ZU, Ahmed W, Arshad H, Zaidi AA (2021) Natural fiber reinforced composites: Sustainable materials for emerging applications. Results Eng 11:100263. 10.1016/j.rineng.2021.100263
3. Rafiq A, Kumar R, Kumar P, Mural S (2023) Tribology International Natural fiber reinforced polymer composites: A comprehensive review of Tribo-Mechanical properties. Tribol Int 189:108978. 10.1016/j.triboint.2023.108978
4. Sari NH, Syafri E, Suteja W, Fatriasari, Karimah A (2023) Comprehensive Characterization Of Novel Cellulose Fiber From Paederia Foetida and Its Modification For Sustainable Composites Application. J Appl Sci Eng 26(10):1399–1408. 10.6180/jase.202310_26(10).0005
5. Sari NH et al (2024) Exploring the impact of water soaking on the mechanical, thermal, and physical properties of Paederia foetida fiber stem biocomposites : A study in sustainable material innovation. Case Stud Chem Environ Eng 10:100977. 10.1016/j.cscee.2024.100977. August
6. Bakar A et al (2023) Exploring the potential of mahogany extract as a natural dye for the coloration of jute fabric. Heliyon 9(9):1–12. 10.1016/j.heliyon.2023.e19464
7. Herlina N, Suteja S, Wardani D, Lokantara IP (2026) Optimizing Mahogany Peel Powder-Polyester Composites for Sustainable Automotive Interior Panels: Effects of Filler Content on Mechanical and Thermal Properties. Mech Adv Compos Struct 13(28):439–450

8. Nazari S, Ivanova TA, Mishra RK, Müller M, Akhbari M, Hashjin ZE (2024) Effect of Natural Fiber and Biomass on Acoustic Performance of 3D Hybrid Fabric-Reinforced Composite Panels. Materilas 17(5695):1–19
9. Alrasheedi NH, Kumar PM, Balaji D, Sathishkumar M (2025) Hybrid natural fiber composites based on cashew apple bagasse and mahogany fruit for multifunctional performance, *J. Mater. Res. Technol.*, vol. 37, no. July, pp. 4739–4751. 10.1016/j.jmrt.2025.07.111
10. Mohammadi M et al (2023) October., Recent progress in natural fiber reinforced composite as sound absorber material, *J. Build. Eng.*, vol. 84, no. p. 108514, 2024. 10.1016/j.jobe.2024.108514
11. Sari NH, Wardana ING, Irawan YS, Siswanto E (2017) Corn husk fiber-polyester composites as sound absorber: Nonacoustical and acoustical properties, *Adv. Acoust. Vib.*, vol. pp. 1–7, 2017. 10.1155/2017/4319389
12. Munshi MR et al (2022) An Experimental Study of Physical, Mechanical, and Thermal Properties of Rattan-Bamboo Fiber Reinforced Hybrid Polyester Laminated Composite. J Nat Fibers 19(7):2501–2515. 10.1080/15440478.2020.1818354
13. Dev B, Repon R, Haji A (2023) Recent progress in thermal and acoustic properties of natural fiber reinforced polymer composites: Preparation, characterization, and data analysis. Polym Compos 44:7235–7297. 10.1002/pc.27633
14. Herlina Sari N, Wardana ING, Irawan YS, Siswanto E (2018) Characterization of the Chemical, Physical, and Mechanical Properties of NaOH-treated Natural Cellulosic Fibers from Corn Husks. J Nat Fibers 15(4):545–558. 10.1080/15440478.2017.1349707
15. Rao HJ et al (2024) Enhancing mechanical performance and water resistance of Careya-Banana fiber epoxy hybrid composites through PLA coating and alkali treatment. J Mater Res Technol 32:4304–4315. 10.1016/j.jmrt.2024.08.190
16. Kumar S, Saha A, Zindani D (2023) Agro-waste-based polymeric composite laminates for aerospace cabin interior and identification of their optimal configuration. Biomass Convers Biorefinery 14(24):31907–31923. 10.1007/s13399-023-04914-2
17. ASTMD 792 (2007) Standard Test Methods for Density and Specific Gravity (Relative Density) of Plastics, in *Anual Book of ASTM Standard*, vol. 14, pp. 1–5
18. Akhyar A, Gani M, Ibrahim F, Ulmi, Farhan A (2024) The influence of different fiber sizes on the flexural strength of natural fiber-reinforced polymer composites, *Results Mater.*, vol. 21, pp. 1–21, Mar. 10.1016/j.rinma.2024.100534
19. Schatzmayr T et al (2026) Impact of a phosphorus-based fireproof treatment on the acoustic performances of bulk hemp fibers. Appl Acoust 249:111287. 10.1016/j.apacoust.2026.111287
20. Rahim FHA, Shah SZH, Megat-yusoff PSM, Hussnain SM, Choudhry RS, Hussain MZ (2024) Mechanical and viscoelastic properties of novel resin-infused thermoplastic tri-block copolymer 3D glass fabric composites. Polym Test 137:108510. 10.1016/j.polymertesting.2024.108510
21. Ruan JQ et al (2023) Multifunctional ultralight nanocellulose aerogels as excellent broadband acoustic absorption materials. J Mater Sci 58(2):971–982. 10.1007/s10853-022-08118-3

22. Aruna M et al (2026) Integration and mechanical and water absorption characteristics of treated natural fiber-titanium nanoparticles embedded polyester composites. Sci Rep 19(9153):1–15
23. Khieng TK et al (2021) A Review on Mechanical Properties of Natural Fibre Reinforced Polymer Composites under Various Strain Rates the as. J Compos Sci 5(130):1–13
24. Neto PS et al (2025) Properties evaluation of polyester composites with fillers for electrical sector applications. J Mater Sci Compos 6(9):1–12
25. Sathishkumar G et al (2025) Experimental study on mechanical performance and microstructural characterization of optimized sisal fiber reinforced polyester composites. Sci Rep 15(36348):1–26
26. Ardiansyah NA, Widodo RD, Nuryanta MI (2026) Flexural performance of HDPE composites reinforced with natural ijuk fibers. J Terap Tek Mesin 7(1):231–239
27. Kumar SS, Shyamala P, Pati PR, Mishra DK (2025) Investigation and machine learning-based prediction of mechanical properties in hybrid natural fiber composites. Sci Rep 15(33700):1–28
28. Daniel D et al (2024) Potential of wood fiber / polylactic acid composite microperforated panel for sound absorption application in indoor environment. Constr Build Mater 444:137750. 10.1016/j.conbuildmat.2024.137750
29. Hindi J, K M, Bhat KS, B M G, Ibrahim A (2025) Physical, Morphological, Tensile, and Thermal Stability Characteristics of Novel Tinospora Cordifolia Natural Fiber. J Nat Fibers 22(1):1–12. 10.1080/15440478.2024.2437539
30. Palani K et al (2025) Characterization of new natural cellulosic fibre extracted from the barks of Trianthema Portulacastrum. Int J Biol Macromol 307:141999. 10.1016/j.ijbiomac.2025.141999
31. Aprilia S, Syamsuddin Y, Amin A, Zuwanna I (2023) Physical, morphological, mechanical and thermal properties of polyester composites reinforced with orientation of purun fiber (Eleocharis dulcis) composition, *South African J. Chem. Eng.*, vol. 47, no. November pp. 338–344, 2024
32. Al A, Bhuiyan N, Kumar A, Hasib A, Rahim N, Uddin S (2025) Effect of chemical treatments on the mechanical and physical properties of kenaf-carbon fiber hybrid epoxy composites, vol. 10, no. November 2026

Figures

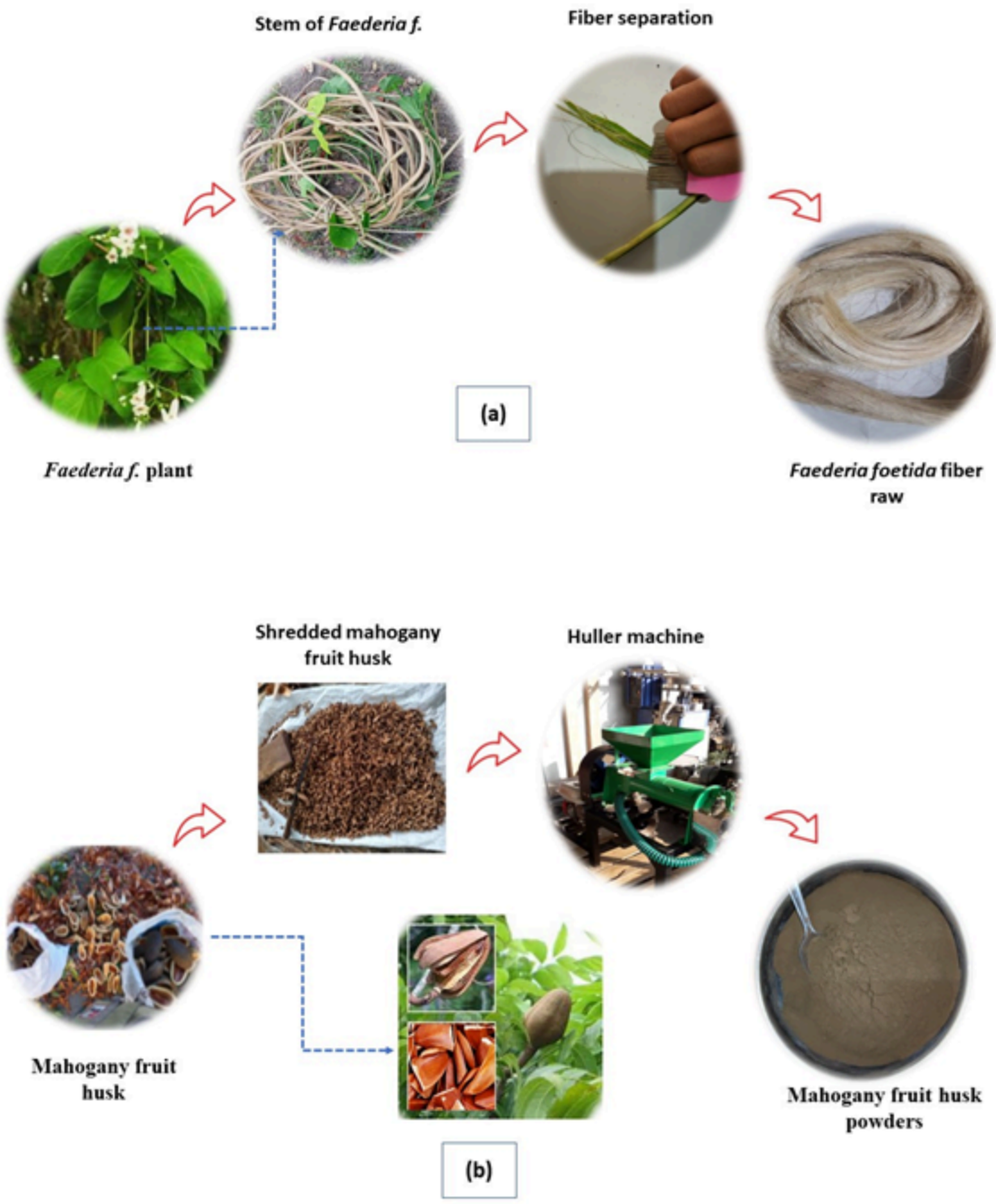


Figure 1

Extraction and preparation of (a) *Faederia foetida*fibers, (b) Mahongany fruit husk powders

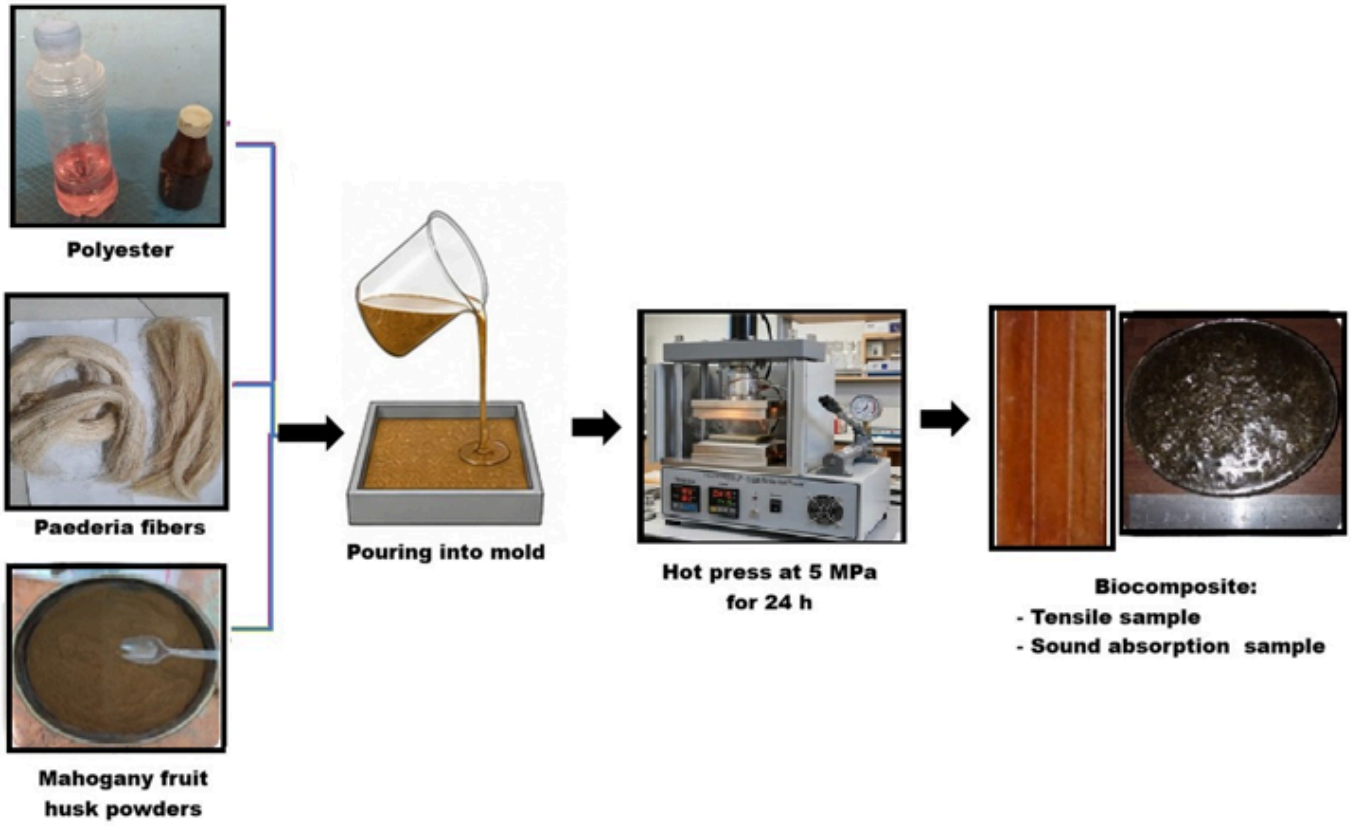


Figure 2

Schematic of PFs/MP biocomposite fabrication

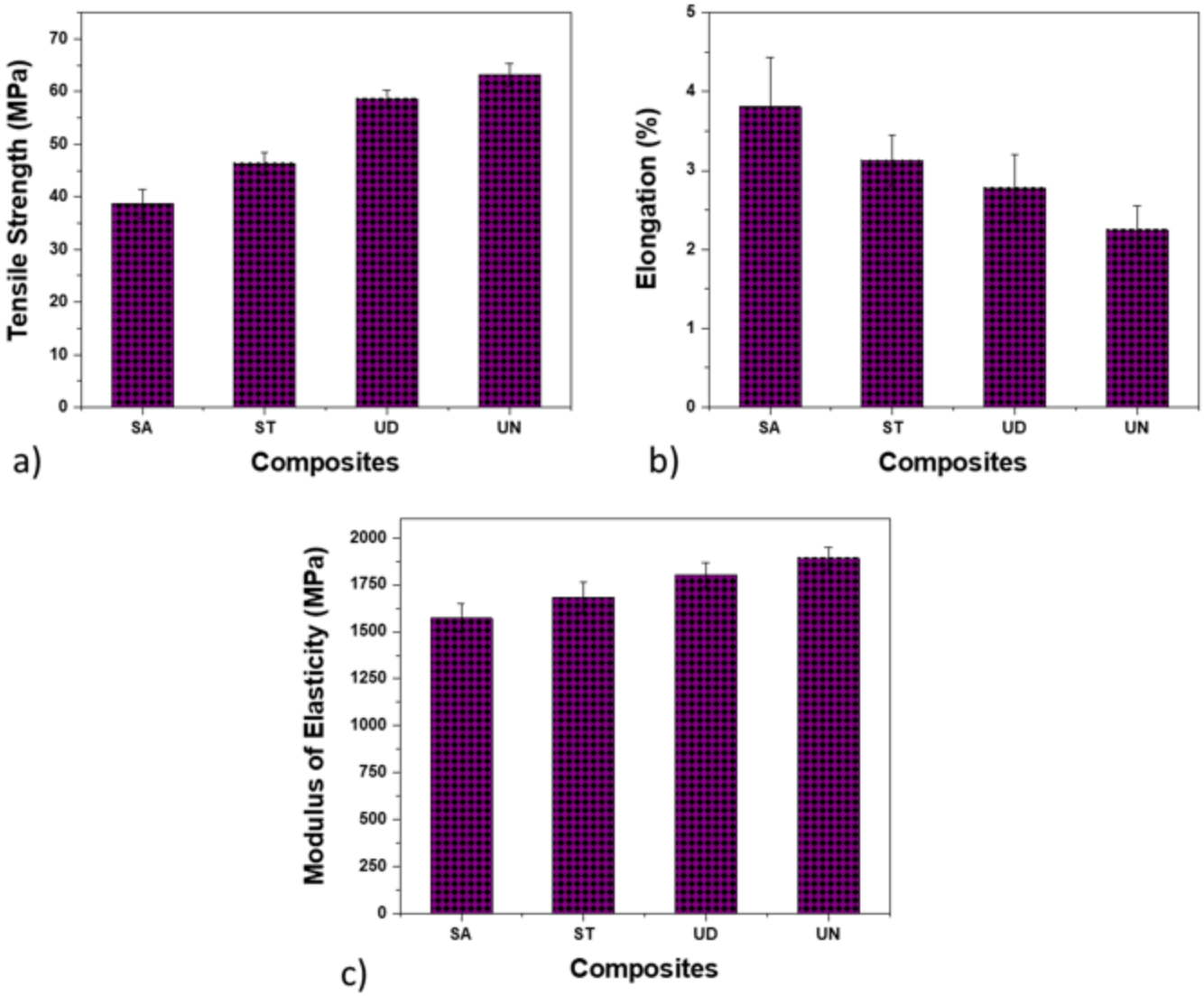


Figure 3

a). Tensile strength, b) elongation, and c) modulus of elasticity of PFs/MP biocomposites

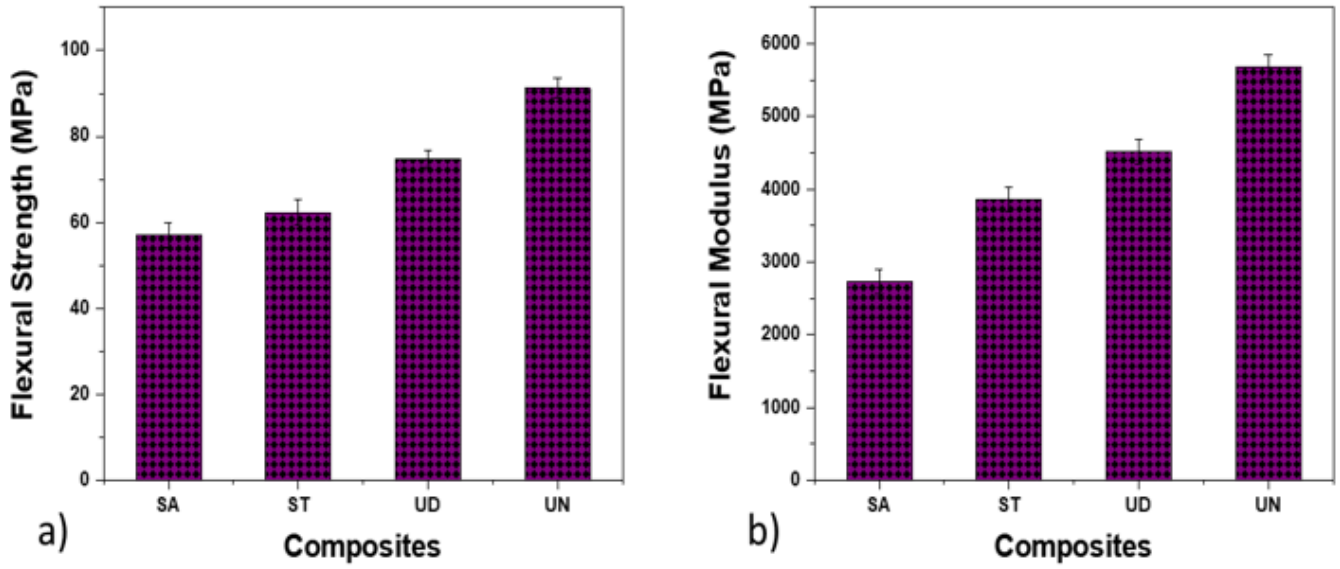


Figure 4

a). Flexural strength, b) modulus of flexural of PFs/MP biocomposites

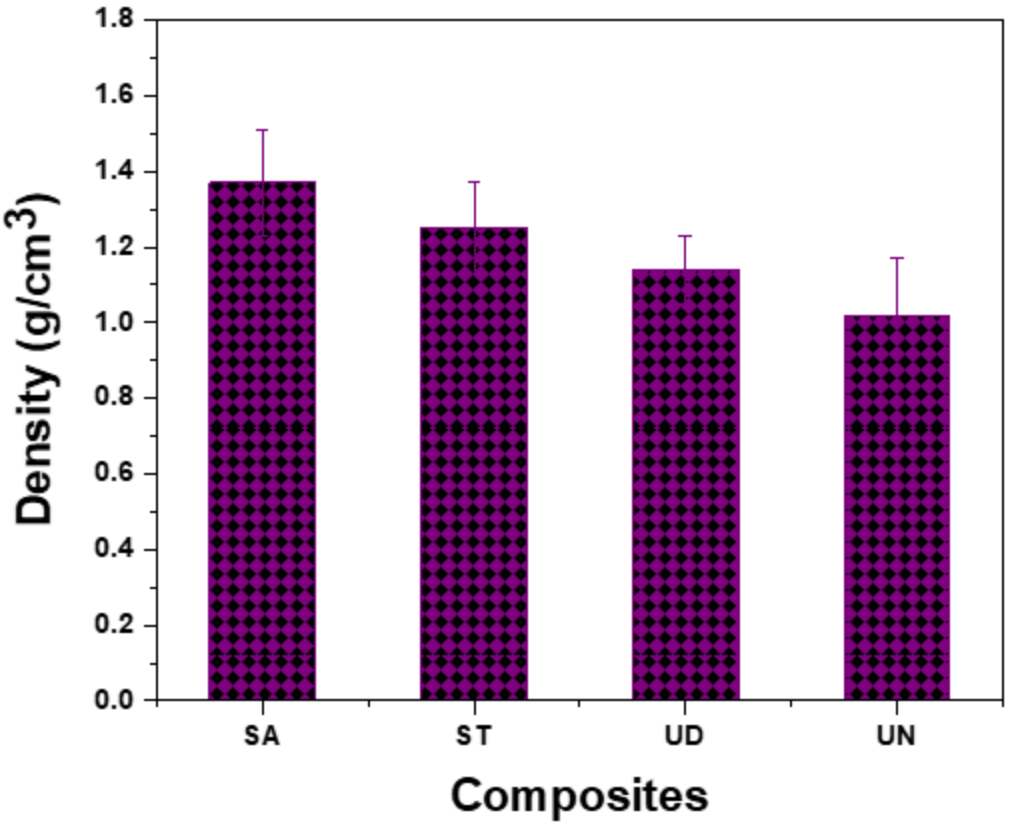


Figure 5

Density of PFs/MP biocomposites

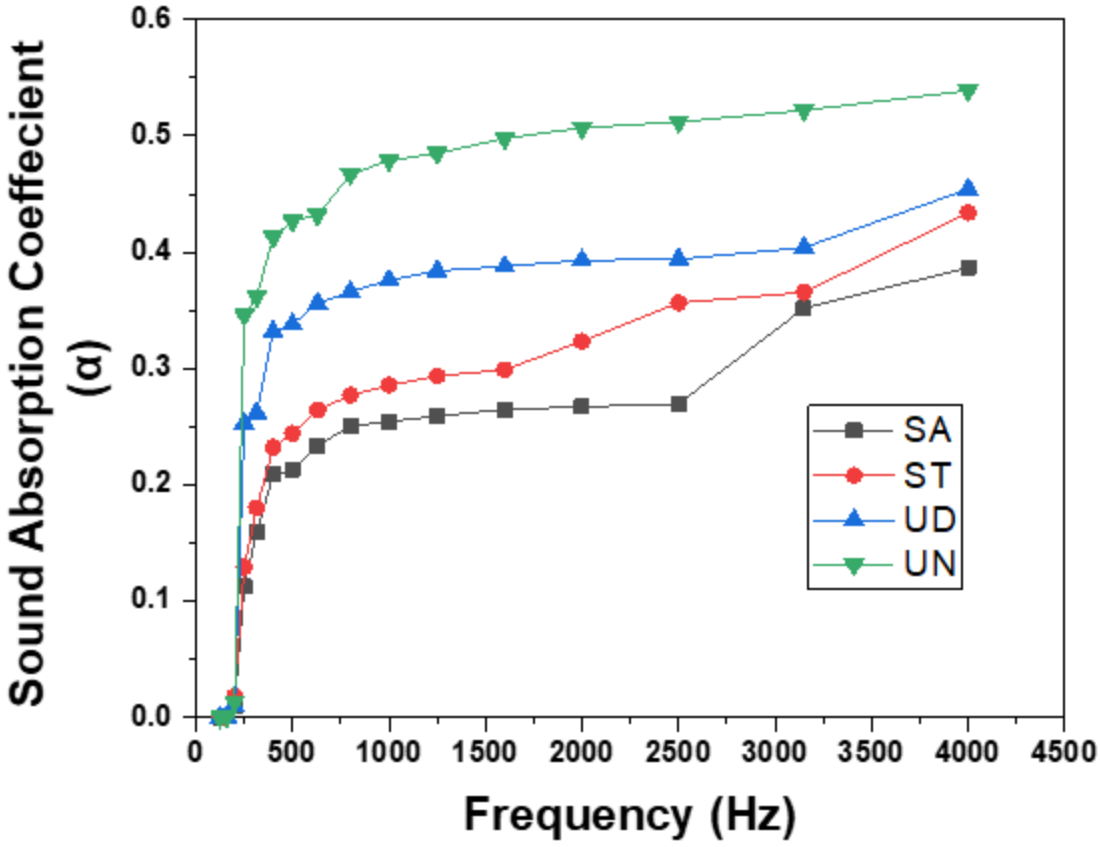


Figure 6

Sound absorption characteristic of PFs/MP biocomposites

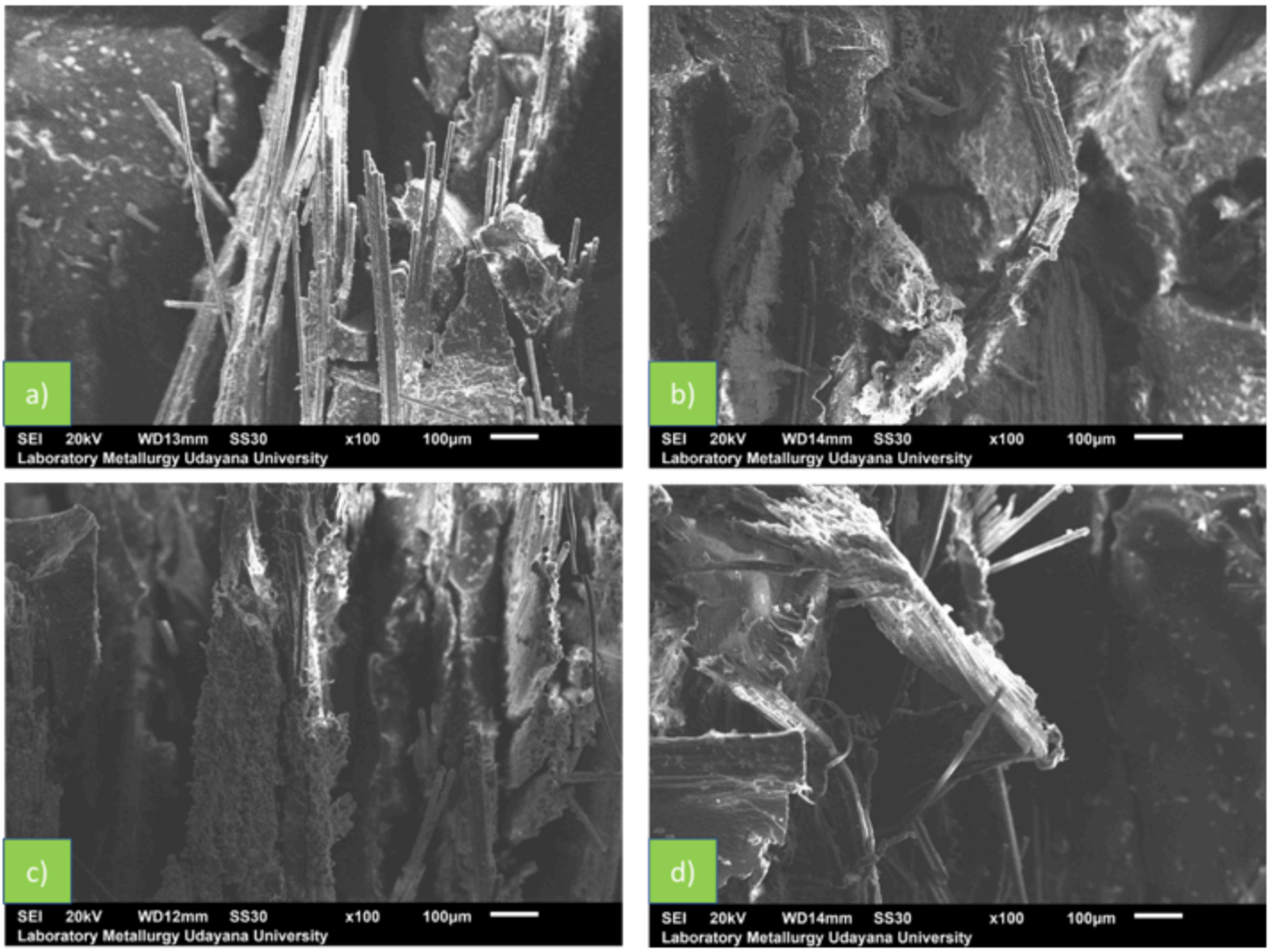


Figure 7

SEM photos of the fracture surface morphology of PFs/MP biocomposites a). SA, b) ST, c) UD, and d) UN

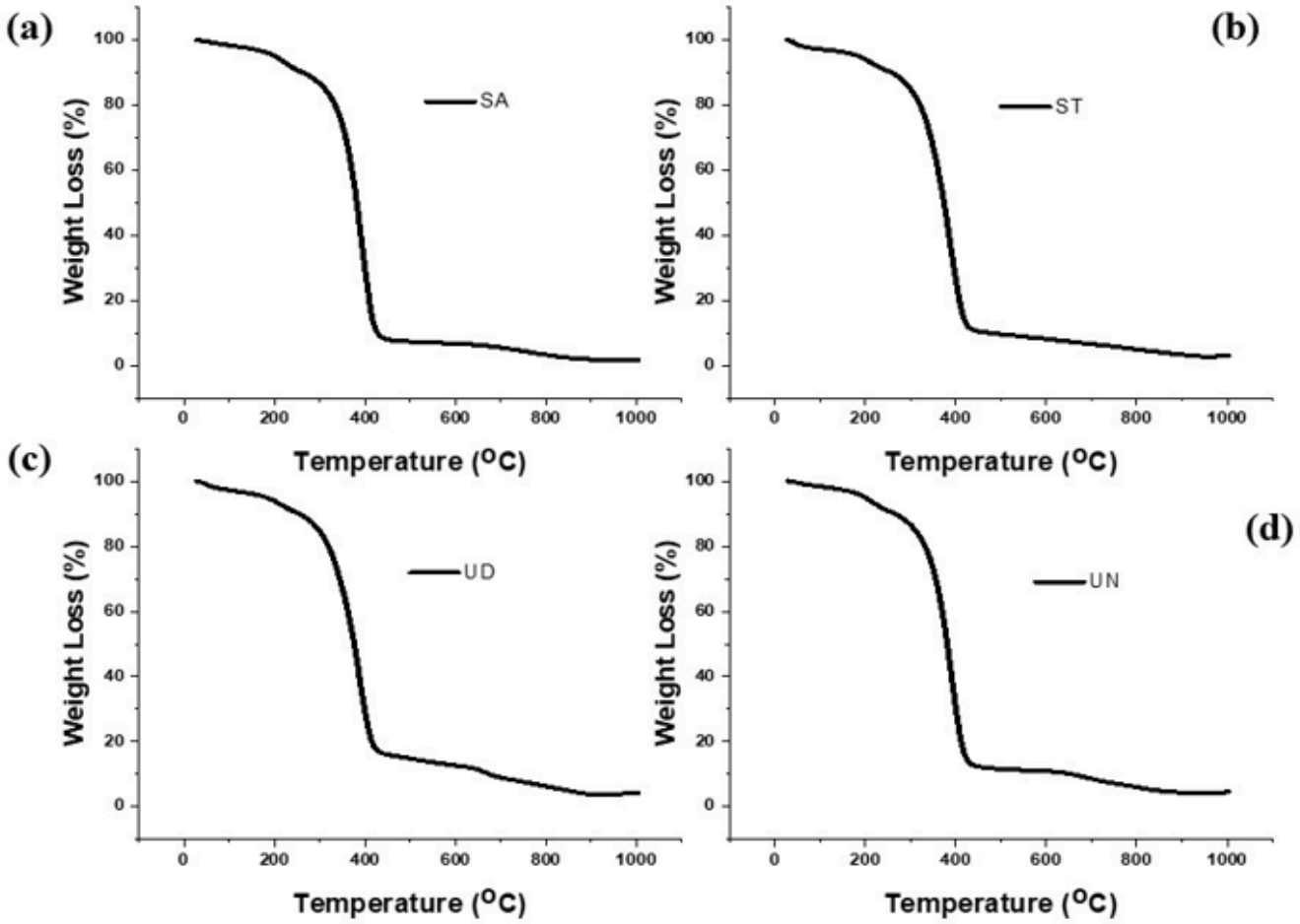


Figure 8

The TGA of PFs/MP biocomposites samples, a) SA, b) ST, c) UD, and d) UN.